Journal of Fluorine Chemistry 129 (2008) 529–534

Contents lists available at ScienceDirect

Journal of Fluorine Chemistry

journal homepage: www.elsevier.com/locate/fluor

Atomic fluorine in cobalt trifluoride thermolysis

Miroslav S. Leskiv [a], Norbert S. Chilingarov [a,*], Julietta V. Rau [a,b], Daniela Ferro [b], Sergey V. Abramov [a], Felix M. Spiridonov [a], Lev N. Sidorov [a]

[a] Chemistry Department of M.V. Lomonosov Moscow State University, 119992 Moscow, Russia
[b] CNR Istituto per lo Studio dei Materiali Nanostrutturati, Piazzale Aldo Moro 5 – 00185 Roma, Italy

ARTICLE INFO

Article history:
Received 17 January 2008
Received in revised form 27 March 2008
Accepted 31 March 2008
Available online 6 April 2008

Keywords:
Atomic and molecular fluorine
Thermolysis of solid fluorinating reagents
Thermal decomposition of solids
Solid-phase fluorination
Mass spectrometry

ABSTRACT

The thermal decomposition of cobalt trifluoride was studied by High Temperature Mass Spectrometry (HTMS). It was ascertained that the rate of atomic fluorine evolution in the gas phase might be increased by adding small amounts of Ni(s) or CoF_2(s) to cobalt trifluoride. Scanning Electron Microscopy combined with Energy Dispersive X-ray spectroscopy (SEM/EDX) was used to determine the morphology and composition of the solid product surface layer formed under different rates of CoF_3(s) thermolysis.

1. Introduction

Cobalt trifluoride has been used for a long time, as a mild fluorinating reagent for the synthesis of organic fluoroderivatives [1,2]. Fluorination occurs on the surface of CoF_3(s) particles to which organic molecules R have been supplied. The reaction product RF_n, formed within the 320–570 K temperature range, can easily be distilled off. In all the fluorination mechanisms discussed in the literature, atomic fluorine is considered to be a participant in the basic stages of the reaction. Possible fluorination routes of some aromatic and heterocyclic compounds are suggested in [3,4].

The evolution of fluorine from the CoF_3(s) crystals is one stage that is common to all the fluorination reactions regardless of the nature of R. This stage is present in the solid-state thermal decomposition reaction of the CoF_3(s). Therefore, the composition of gaseous products of the CoF_3(s) thermolysis and factors affecting its rate are important for understanding the mechanism of more complex reactions such as solid-phase fluorination.

The evaporation of CoF_3(s) was studied previously [5–8], wherein correlations between the enthalpies of sublimation (Eq. (1)):

$$CoF_3(s) \rightarrow CoF_3(g) \quad (1)$$

and dimerization (Eq. (2)):

$$2CoF_3(g) \rightarrow Co_2F_6(g) \quad (2)$$

were established.

In contrast, the thermal decomposition of CoF_3(s) has not been investigated in detail. In the first mass-spectrometric study [5], besides sublimation products, CoF_3 and Co_2F_6, thermal decomposition products were found: atomic and molecular fluorine (in the gas phase), and cobalt difluoride (in the solid-phase). These results showed that the cobalt trifluoride sublimation is accompanied by the following decomposition (Eq. (3)):

$$CoF_3(s) \rightarrow CoF_2(s) + F(g) \quad (3)$$

The aim of this work is to study the kinetic factors responsible for the evolution of atomic fluorine upon the thermal decomposition of CoF_3(s), and to find the conditions that drastically increase the atomic fluorine partial pressure P(F). The composition of gaseous products under different conditions of CoF_3(s) evaporation was registered by the High Temperature Mass Spectrometry (HTMS) method. The morphology and composition of surface layers were determined by Scanning Electron Microscopy (SEM) combined with an Energy Dispersive X-ray (EDX) module.

* Corresponding author. Tel.: +7 495 939 54 63; fax: +7 495 939 12 40.
E-mail address: nsc@phys.chem.msu.ru (N.S. Chilingarov).

0022-1139/$ – see front matter © 2008 Elsevier B.V. All rights reserved.
doi:10.1016/j.jfluchem.2008.03.012

Table 1
Atomic fluorine pressures upon pure CoF_3(s) thermal decomposition {Ni/NiF_2}

N	T (K)	t (h)	P(F) (atm)	$\bar{P}$(atm)	ΔP (atm)
1.1.	698	5	2.8×10^{-8}; 4.0×10^{-8}; 3.2×10^{-8}; 3.3×10^{-8}; 2.8×10^{-8}; 2.8×10^{-8}	3.2×10^{-8}	0.4×10^{-8}
1.2.	730	7	1.7×10^{-7}; 2.1×10^{-7}; 3.1×10^{-7}; 2.4×10^{-7}; 1.8×10^{-7}; 2.8×10^{-7}; 3.5×10^{-7}	2.5×10^{-7}	0.6×10^{-7}
1.3.	730	2	2.1×10^{-7}; 1.8×10^{-7}		
1.4.	758	2	9.0×10^{-7}; 9.1×10^{-7}		
1.5.	758	5	7.4×10^{-7}; 6.6×10^{-7}; 9.5×10^{-7}; 7.4×10^{-7}; 8.6×10^{-7}	7.9×10^{-7}	0.9×10^{-7}
2.1.	735	1	8.3×10^{-7}		
2.2.	765	6	2.9×10^{-6}; 3.7×10^{-6}; 2.6×10^{-6}; 3.7×10^{-6}; 3.2×10^{-6}	3.2×10^{-6}	0.4×10^{-6}
3.1.	734	2	5.1×10^{-7}		
3.2.	776	1	4.4×10^{-6}		
3.3.	778	7	5.9×10^{-6}; 6.5×10^{-6}; 3.8×10^{-6}; 4.0×10^{-6}; 4.8×10^{-6}	5.0×10^{-6}	1.0×10^{-6}
3.4.	776	1	4.9×10^{-6}		
3.5.	772	5	4.4×10^{-6}; 2.7×10^{-6}; 3.8×10^{-6}; 5.4×10^{-6}	4.1×10^{-6}	0.8×10^{-6}
3.6.	776	5	5.5×10^{-6}; 5.1×10^{-6}; 4.3×10^{-6}; 3.0×10^{-6}	4.5×10^{-6}	0.8×10^{-6}

$\bar{P}$ and ΔP were calculated according the formulas: $\bar{P} = (1/n)\times\sum P(F)$; $\Delta P = (1/n)\times\sum(|P(F)-\bar{P}|)$.

2. Results and discussion

2.1. Evaporation of pure CoF_3(s)

Regardless of pure CoF_3(s) evaporation conditions, the sublimation products, CoF_3 and Co_2F_6, and thermal decomposition products, F and F_2, were fixed in the gas phase by the HTMS method. In all experiments a solid pink residue was found after evaporation. Using X-ray powder diffraction, it was identified as CoF_2(s). Most likely, atomic fluorine is the primary product of CoF_3(s) decomposition, and cobalt trifluoride thermolysis occurs according to reaction (3). Molecular fluorine seems to be the product of F atoms recombination. Because the free path of the vapor species exceeds the linear dimensions of the reaction vessel (Knudsen cell) at pressures used ($P \leq 10^{-4}$ atm, 1 atm = 101,325 Pa), molecular fluorine is likely to be the product of heterogeneous recombination of F atoms adsorbed on the sample surface.

The pressures P(F) measured at temperatures T within time intervals Δt under evaporation of pure CoF_3(s) from {Ni/NiF_2} and {Pt} cells are presented in Tables 1 and 2, respectively. The average pressures ($\bar{P}$) and the average deviations (ΔP) of P(F) values from $\bar{P}$ are deduced. Irrespective of the cell material, the pressures P(F) obtained at the same temperature are very close. Note, the time intervals between the sets of P(F) values 1.2 and 1.3, 1.4 and 1.5 (Table 1), 1.2 and 1.6 (Table 2) are 7, 3, and 8 h, respectively. An example of the pressure P(F) invariance with time (data 1.2 and 1.3, Table 1) is demonstrated in Fig. 1. The pressures P(F) obtained in different runs at the same temperature vary within a factor of two. A stepped temperature increase leads to a growth of the pressure P(F).

Atomic fluorine pressures in the pure CoF_3(s) vapor were obtained in [8] by the HTMS method. Pressure P(F) at 723 K was calculated from the mass of the formed CoF_2(s) (3.9×10^{-7} atm), and from mass-spectrometric measurements (5.2×10^{-7} atm). A satisfactory agreement between these pressures and the values presented in Tables 1 and 2 can be seen.

2.2. The realization of CoF_3(s) thermolysis high rate

The experimental procedure used in our study allowed us not only to determine P(F), but also to search for thermolysis conditions that lead to the enhanced partial pressure of atomic fluorine at constant T. Obviously, this goal can be achieved, if we can increase the thermolysis rate, while simultaneously minimizing the atomic fluorine loss. We attempted to solve this using a reducer – nickel metal.

Introduction of Ni(s) into the system leads to solid-phase fluorination (Eq. (4)):

$$2CoF_3(s) + Ni(s) \rightarrow 2CoF_2(s) + NiF_2(s) \quad (4)$$

The Gibbs energy of this reaction is essentially negative, $\Delta_r G^\circ(4) = -428$ kJ mol^{-1} (T = 700 K) [9]; therefore, the rate of CoF_3(s) decomposition should be rather high. However, a nickel surface rapidly passivates, and the rate of atomic fluorine loss decreases. Thus, if the high rate of CoF_3(s) decomposition according to the reaction (3) remains unchanged, the partial pressure of atomic fluorine in the system could increase.

Table 2
Atomic fluorine pressures upon pure CoF_3(s) thermal decomposition {Pt}

N	T (K)	t (h)	P(F) (atm)	$\bar{P}$(atm)	ΔP (atm)
1.1	694	3	7.9×10^{-8}; 1.3×10^{-7}; 9.8×10^{-8}	1.0×10^{-7}	0.2×10^{-7}
1.2.	714	3	1.5×10^{-7}; 1.6×10^{-7}; 2.0×10^{-7}	1.7×10^{-7}	0.2×10^{-7}
1.3.	734	3	5.7×10^{-7}; 3.9×10^{-7}; 6.2×10^{-7}	5.3×10^{-7}	0.9×10^{-7}
1.4.	755	2	1.2×10^{-6}; 1.4×10^{-6}; 1.4×10^{-6}	1.3×10^{-6}	0.1×10^{-6}
1.5.	775	1	3.2×10^{-6}		
1.6.	714	1	1.7×10^{-7}		
2.1	714	3	1.8×10^{-7}; 1.4×10^{-7}; 1.1×10^{-7}	1.4×10^{-7}	0.2×10^{-7}
2.2.	734	3	1.4×10^{-7}; 3.1×10^{-7}; 2.5×10^{-7}	2.3×10^{-7}	0.6×10^{-7}
2.3.	754	3	1.4×10^{-6}; 1.0×10^{-6}; 1.3×10^{-6}	1.2×10^{-6}	0.2×10^{-6}
2.4.	773	3	4.5×10^{-6}; 5.5×10^{-6}; 6.9×10^{-6}	5.6×10^{-6}	0.8×10^{-6}
2.5.	793	2	1.6×10^{-5}; 1.3×10^{-5}		
3.1.	778	3	4.0×10^{-6}; 4.3×10^{-6}; 3.6×10^{-6}	4.0×10^{-6}	0.2×10^{-6}

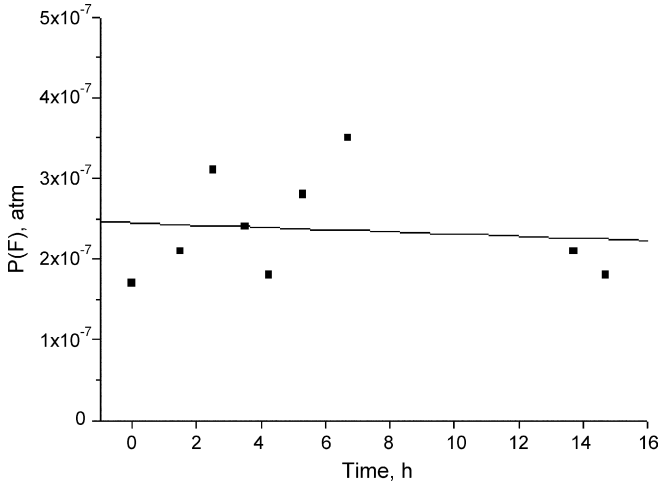

Fig. 1. The pressure P(F) invariance with time upon pure CoF_3(s) evaporation; {Ni/NiF_2}, T = 730 K.

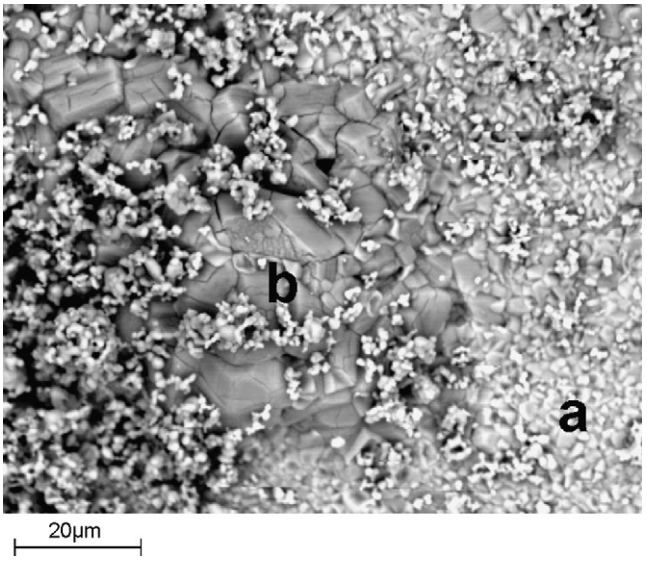

Fig. 3. The SEM image of nickel plate surface after the 40 h of evaporation of the CoF_3(s)–Ni(s) mixture; {Ni/NiF_2}, T = 733 K.

When cobalt trifluoride evaporates in the presence of nickel, the atomic fluorine partial pressure is essentially higher than in the saturated vapor over pure CoF_3(s). The time dependence of the pressure, P(F), under isothermal evaporation of the CoF_3(s)–Ni(s) mixture ({Ni/NiF_2}, T = 733 K, m(CoF_3)/m(Ni) = 2.3) is shown in Fig. 2. According to our data the atomic fluorine pressure in the CoF_3(s) saturated vapor at 733 K is lower, 2.1×10^{-7} atm.

To interpret our experimental data, one should consider that thermal decomposition solid-phase reactions start in reaction centers or nuclei [10]. In the presence of nickel, these nuclei can be formed in the defects of specimen crystals upon the intensive emission of F atoms from these CoF_3 crystals. The nuclei are likely concentrated mainly on CoF_3(s)–Ni(s) interphase boundaries. The concentration of thermolysis centers is thus higher as compared with those formed from CoF_3(s) evaporation without nickel. As a result, the partial pressure P(F) in the CoF_3(s) saturated vapor becomes more than one order of magnitude higher once nickel is added. The monotonic increase in P(F) during the 15 h after the beginning of evaporation (Fig. 2) can be explained by the passivation of the nickel surface and the corresponding decrease in the rate of atomic fluorine loss at a constant thermolysis rate. The subsequent slow decrease in P(F) reflects the evolution of the system to the final thermodynamically stable state, namely, the equilibrium between the CoF_2(s), NiF_2(s) and Ni(s) phases. The corresponding limit for P(F) is 1.3×10^{-22} atm (T = 733 K) [9].

SEM data show that surface layers with similar morphology are formed on nickel plates after 6 and 40 h of fluorination (T = 733 K). The main part of the surface (Fig. 3) is occupied by particles (a) having virtually unchanged composition, n(F)/n(Co). The presence of Co, F, and O atoms was detected in comparatively large crystals (b). The concentration of Ni atoms depended on the thickness of analyzed layer. For example, the n(Ni)/n(Co) ratio in particles (a) decreased from 0.6 to 0.03 after 6 and 40 h of fluorination, respectively.

The use of nickel is not the only way to increase the rate of reaction (3). High pressures of atomic fluorine could also be obtained after adding a small amount of CoF_2(s) to cobalt trifluoride. Atomic fluorine pressures in the vapor over the CoF_3(s)–CoF_2(s) (<10 mol%) system (T = 733 K {Ni/NiF_2}) are given in Fig. 4. The high pressure of atomic fluorine and, therefore, the high rate of cobalt trifluoride thermolysis in the CoF_3(s)–CoF_2(s) system can also be due to a large number of formed nuclei which act as thermolysis reaction centers. It seems likely that CoF_2

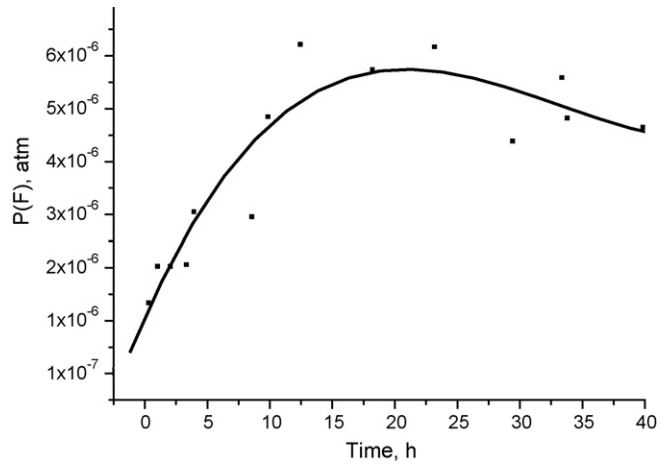

Fig. 2. The time dependence of P(F) upon the CoF_3(s)–Ni(s) system evaporation; {Ni/NiF_2}, T = 733 K, m(CoF_3)/m(Ni) = 2.3.

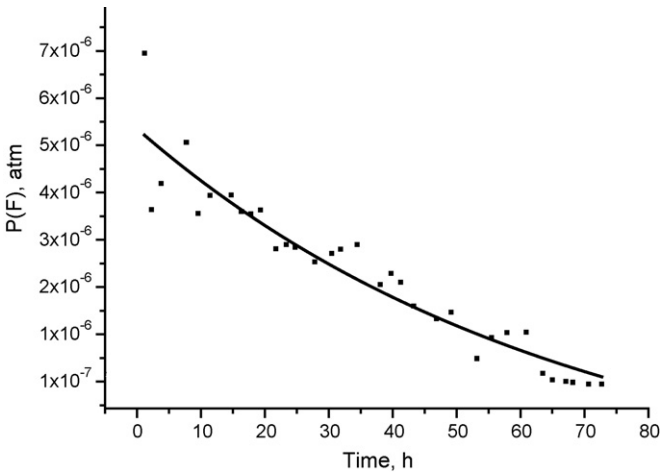

Fig. 4. The time dependence of P(F) upon the CoF_3(s)–CoF_2(s) mixture evaporation; {Ni/NiF_2}, T = 733 K.

Table 3
Experimental and calculated equilibrium constants $K_P(3)$ at $T = 733$ K

System	$K_P(3)$ (atm)
[9]	2×10^{-7}
$CoF_3(s)$–$CoF_2(s)$[a] {Ni/NiF_2}	4×10^{-6}
$CoF_3(s)$–$CoF_2(s)$[b] {Ni/NiF_2}	3×10^{-6}
$CoF_3(s)$–$CoF_2(s)$ {Pt}	3×10^{-6}

[a] Residue after the $CoF_3(s)$ evaporation.
[b] Annealed $CoF_2(s)$ sample (Aldrich Chemical Co.).

particles are a part of the nuclei, and thermolysis occurs on the $CoF_3(s)$–$CoF_2(s)$ interphase. The slow decrease of $P(F)$ with time (Fig. 4) is connected with the evolution of the system towards an equilibrium state. The effect does not depend on cell material ({Ni/NiF_2} or {Pt}), or on the prehistory of $CoF_2(s)$. High rates of thermolysis were obtained for the annealed $CoF_2(s)$ sample (Aldrich Chemical Co), and for the $CoF_2(s)$ residue after $CoF_3(s)$ evaporation.

The rate of the $CoF_3(s)$ thermal decomposition is influenced by the shape and size of the solid product particles. The product of the pure $CoF_3(s)$ thermolysis consisted of spherical particles ranging in size from 0.5 to 3.0 μm (Fig. 5a). Particles with irregular form having sizes of up to ~8 μm prevailed in the solid residue after the evaporation of the $CoF_3(s)$–$CoF_2(s)$ (≤10 mol%) mixture (Fig. 5b). This difference can be explained by the aggregation of small CoF_2 particles formed from rapid cobalt trifluoride thermolysis.

Pressures $P(F)$ over the $CoF_3(s)$–$CoF_2(s)$(10 mol%) systems allow the calculation of equilibrium constants $K_P(3)$ assuming that the activities of cobalt di- and trifluoride are equal to unity. As can be seen from Table 3, deviations ($P(F)$ increase) from equilibrium ($K_P(exp) > K_P(eq)$) take place independently of cell material. Note, that under equilibrium conditions, an increase in CoF_2 activity can only lead to a decrease in atomic fluorine partial pressure.

In Table 4 the experimental pressures $P(F)$ and $P(F_2)$, equilibrium constants of the reaction (Eq. (5)):

$$F_2(g) \rightarrow 2F(g) \quad (5)$$

and the $\{P(F)/P(F_2)\}$ ratios at $T = 733$ K are shown and compared with values calculated using the IVTANTHERMO database [9]. Again considerable deviations from equilibrium were found in all systems where high rates of thermolysis had been realized.

The absence of an equilibrium in reaction (5) under a high rate of thermal decomposition was found earlier [11] in a study of $TbF_4(s)$ thermolysis. This process is accompanied by a peculiar change in the $CoF_3(s)$ structure: F atoms leave the lattice, and the concentration of vacancies (on fluorine) in the structure increases. The CoF_3 phase with F vacancies [$CoF_{3-\delta}$], can be considered as an intermediate phase. With time, the surface layer of decomposing CoF_3 particles becomes saturated with vacancies. The final solid product of thermolysis, $CoF_2(s)$, is formed by a structural transformation of [$CoF_{3-\delta}$] phase once a critical vacancies concentration is attained. The existence of the vacancy structure in the surface layer leads to the low rate of heterogeneous recombination, and, as a result, to the kinetic stability of the atomic state of fluorine and to a deviation from equilibrium in the $2F \rightarrow F_2$ reaction.

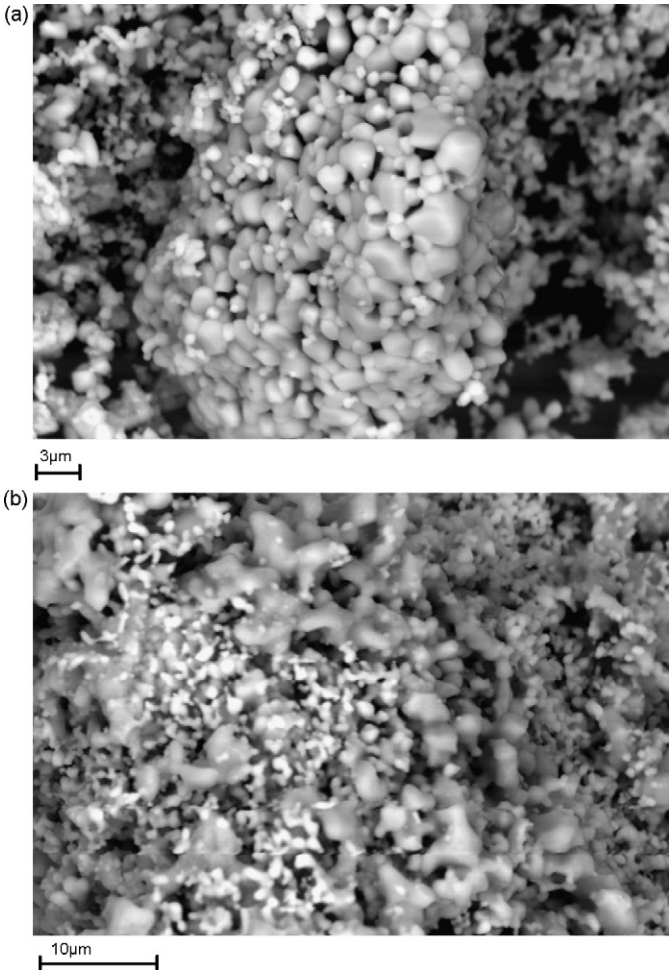

Fig. 5. The SEM image of the residue after CoF_3 decomposition has been completed {Pt}. (a) Pure $CoF_3(s)$; $T = 670/770$ K; (b) $CoF_3(s)$–$CoF_2(s)$ (≤10 mol%) mixture; $T = 733$ K.

The vacancy structure hypothesis gives us a rough idea about the solid-phase fluorination mechanism. Organic substances R are strong reducers, so volatile RF products are readily formed at relatively low temperatures. The depletion of F atoms from CoF_3 phase leads to the formation of vacancy structures in the surface layer. Under such conditions, F atoms do not recombine and are the main fluorinating reagent. It is believed that the vacancy structure is included in the fluorination mechanism: F atoms pass from cobalt trifluoride to R molecules inside of complexes [R···$CoF_{3-\delta}$] which are formed at the juncture of R molecules on free valences (vacancies) of the surface layer. After the reaction is completed and

Table 4
Experimental and equilibrium data for reaction (5) at $T = 733$ K

System	$P(F)$ (atm)	$P(F_2)$ (atm)	$K_P(5)$ (atm) (exp)	$K_P(5)$ (atm) (eq)	$P(F)/P(F_2)$ (exp)	$P(F)/P(F_2)$ (eq)
$CoF_3(s)$ {Pt}	5.7×10^{-7}	3.3×10^{-8}	9.9×10^{-6}	7.2×10^{-6}	17.3	12.9
$CoF_3(s)$–$CoF_2(s)$[a] {Ni/NiF_2}	7.0×10^{-6}	1.5×10^{-7}	3.3×10^{-4}	7.2×10^{-6}	46.7	1.6
$CoF_3(s)$–$CoF_2(s)$[b] {Ni/NiF_2}	3.1×10^{-6}	1.1×10^{-7}	8.7×10^{-5}	7.2×10^{-6}	28.2	3.0
$CoF_3(s)$–$CoF_2(s)$[a] {Pt}	2.8×10^{-6}	1.1×10^{-7}	6.9×10^{-5}	7.2×10^{-6}	25.5	3.2
$CoF_3(s)$–Ni(s) {Ni/NiF_2}	4.5×10^{-6}	2.0×10^{-7}	1.1×10^{-4}	7.2×10^{-6}	22.5	2.2

[a] Residue after the $CoF_3(s)$ evaporation.
[b] Annealed $CoF_2(s)$ sample (Aldrich Chemical Co.).

the complex decomposed, the fluorination product, RF, evolves into the gas phase.

2.3. About CoF_4^+ ions molecular precursors

The data obtained here allow one to ascertain whether CoF_4 molecules are the precursors of CoF_4^+ ions registered during the investigation of all the systems. As pointed out in [12], cobalt tetrafluoride pressure is proportional to atomic fluorine pressure. The pressures $P(F)$ measured in the investigated systems differ by an order of magnitude. Analysis of the experimental data evidenced the following peculiarity: CoF_4 pressures calculated using CoF_4^+ ion intensities are independent of atomic fluorine pressures. Therefore, one can assume that dimer Co_2F_6 is the most likely precursor of the CoF_4^+ ions. Calculations show that the $I(CoF_4^+)/I(Co_2F_5^+)$ ratio in the mass-spectra of all systems is equal to $0.04 \div 0.05$.

3. Conclusion

The cobalt trifluoride thermal decomposition was studied by the High Temperature Mass Spectrometry method. The partial pressures $P(F)$ and $P(F_2)$ were measured. Conditions that increase the rate of $CoF_3(s)$ thermolysis were found. It was ascertained that at high rates of thermolysis the equilibrium between atomic and molecular fluorine is not attained. The surface layers formed under different thermolysis rates were investigated by Scanning Electron Microscopy.

4. Experimental

4.1. HTMS investigation of the gas phase

4.1.1. Method and apparatus

The fundamentals of HTMS have been described in detail in [13]. A magnetic mass-spectrometer MI-1201 (90°, $r = 200$ mm, resolution 300) with an ion source, modified for high temperature investigation was used. The specimen was heated in an effusion cell. A molecular beam of the saturated vapor components entered the ion source. Positive ions formed under electron ionization ($U_{ion} = 65$ V) were accelerated to 3 keV, separated in the uniform magnetic field according to m/e ratios, and passed to the collector (Faraday cup). The "useful" part of signal originating from the saturated vapor components, was separated from the background by a movable shutter installed between the effusion cell and the ionization chamber. This part of the signal was used for the partial pressure calculation according to (Eq. (6)):

$$P_j = k \times (Q_j)^{-1} \sum (I_{ij}) \times T \quad (6)$$

where P_j is the partial pressure of component j (atm); k is the sensitivity constant (atm $\times$ Å^2 $\times$ V^{-1} $\times$ K^{-1}); Q_j is the electron impact ionization cross-section of molecule j, calculated according to the additivity rule (Å^2); $\Sigma(I_{ij})$ is the total current of ions i, formed under the ionization of molecules j (V); T is the temperature (K).

4.1.2. Evaporation procedure

Two ways of evaporating $CoF_3(s)$ were used. Under isothermal evaporation the cell temperature was kept constant (the actual temperature differed from nominal by not more than $\pm$ 1 K). In the second way, the cell temperature was increased stepwise ($\Delta T = 20$ K).

Platinum {Pt}, and nickel {Ni/NiF_2}, cells were used for evaporation. Diameters of the effusion orifices were 0.30 mm and 0.37 mm, respectively. The nickel cell was preliminarily passivated by molecular fluorine at $T = 740$ K and $P(F_2) = 5$ atm for $\sim$10 h.

The temperature of the effusion cell was adjusted by a KT-0203 temperature controller and measured by a Pt-Pt/Rh(10%) thermocouple attached to the cell cover.

4.1.3. Measurement procedure

In all experiments, typical mass spectra consisted of F^+, HF^+, F_2^+, CoF_n^+($n = 0$–4) and $Co_2F_k^+$($k = 0$–6) ions. Ratios of CoF_n^+($n = 0$–3) and $Co_2F_k^+$($k = 0$–6) signals unambiguously indicated the presence of CoF_3 and Co_2F_6 molecules in the gas phase. Each measurement included registration of the "useful" parts of CoF_3^+, $Co_2F_5^+$, CoF_4^+, F^+, and F_2^+ signals.

For all investigated systems, the enthalpies of CoF_3 sublimation calculated applying the second law to the experimental data, were in good agreement with the literature data. This fact can be considered as unambiguous evidence of $P(CoF_3) = P^\circ(CoF_3)$ equality. Therefore, the sensitivity constant k and the partial pressures of the saturated vapor components were calculated according to the Eq. (6) using the intensities of the measured signals.

To determine the partial pressure of atomic fluorine, the contributions of fragment ions F^+ originating from the CoF_3 ionization [8], F_2 and HF molecules [14] to the measured F^+ signal were taken into account. $P(F)$ being calculated only if a part of the F^+ signal corresponding to F atoms was not less than one half of the total F^+ signal. Thus, the accuracy of $P(F)$ is estimated to be within a factor of two.

4.2. SEM/EDX investigations

Analyses were carried out using a LEO 1450 VP Scanning Electron Microscope. The SEM apparatus was coupled with a system for microanalysis (Energy Dispersive X-ray) INCA 300 that allowed us to perform a qualitative/quantitative analysis of the elements starting from atomic number 5 (Boron) with a sensitivity of about 0.2%. By means of the EDX analysis the composition of the surface layers was determined. Taking into account that the penetration depth depends on a series of factors including atomic number and sample density, the attribution of a detected stoichiometry to a determinate phase is limited by a possible contribution of a different composition of the inner layers. This technique allowed us to determine the elemental composition, and so the attribution of an atomic species to a compound is not precise. For these reasons, we took into account only the information concerning the change in the surface layer composition dependent on the conditions of their formation. The validity of this approach was demonstrated in the investigation of indium oxide films, InO_x [15]: measured $n(F)/n(Co(O)/n(F)/n(Co(In)$ ratios exceeded stoichiometric ones, but followed correctly the films composition dependence on the oxygen pressure.

4.3. Materials

$CoF_3(s)$ and $CoF_2(s)$ (>98% purity) samples were supplied by the Aldrich Chemical Co. To study the $CoF_3(s)$–Ni(s) system, nickel plates, 5 mm $\times$ 5 mm $\times$ 0.2 mm, were used.

Since cobalt trifluoride is hygroscopic and hydrolyzes very quickly, all systems with $CoF_3(s)$ were stored and loaded into the effusion cell inside a dry box (with the P_4O_{10} desiccant) in a high purity argon (Ar $\geq$ 99.998%, $O_2 \leq$ 0.0002%, $H_2O \leq$ 0.0003%) atmosphere.

Acknowledgements

The authors gratefully acknowledge Prof. B.V. Romanovskiy for useful discussions of the study subject; Dr. Nelly V. Chelovskaya for help in translating the manuscript, and for many useful comments.

This work was supported by the Russian Foundation for Basic Research (project 05-03-32916a).

References

[1] M. Stacey, J.C. Tatlow, in: M. Stacey, J.C. Tatlow, A.G. Sharpe (Eds.), Advances in Fluorine Chemistry, vol. 1, Butterworths Sci. Publ., London, 1960, pp. 166–198.
[2] J.C. Tatlow, J. Fluorine Chem. 75 (1995) 7–34.
[3] J. Burdon, I.W. Parsons, J.C. Tatlow, Tetrahedron 28 (1972) 43–52.
[4] R.D. Chambers, D.T. Clark, T.F. Holmes, W. Musgrave, R. Kenneth, I. Ritchie, J. Chem. Soc. Perkin I (1974) 114–125.
[5] J.V. Rau, N.S. Chilingarov, L.N. Sidorov, Proc. 14th Int. Mass Spectrometry Conf., August 25–29, 1997, Tampere, Finland, In: E.J. Karjalainen, A.E. Hesso, J.E. Jalonen, U.P. Karjalainen (Eds.), Advances in Mass Spectrometry, vol. 14, Elsevier, Helsinki, 1998, F015260/1-F015260/6.
[6] J.V. Rau, N.S. Chilingarov, L.N. Sidorov, Rapid Commun. Mass Spectrom. 11 (1997) 1977–1979.
[7] G. Balducci, B. Brunetti, V. Piacente, J. Alloys Compounds 260 (1997) 56–58.
[8] A. Popovic, A. Lesar, J.V. Rau, L. Bencze, Rapid Commun. Mass Spectrom. 15 (2001) 749–757.
[9] IVTANTHERMO, Database on thermodynamic properties of individual substances, Developed in THERMOCENTER of the Russian Academy of Science, CRC Press, Boca Raton, 1993.
[10] D. Young, Decomposition of solids, Pergamon press, Oxford, 1966.
[11] N.S. Chilingarov, J.V. Rau, L.N. Sidorov, L. Bencze, A. Popovic, V.F. Sukhoverhov, J. Fluorine Chem. 104 (2000) 291–295.
[12] N.S. Chilingarov, E.V. Skokan, J.V. Rau, L.N. Sidorov, Russ. J. Phys. Chem. (English transl. from Zhurnal Fizicheskoi Khimii) 66 (1992) 1389–1393.
[13] M.G. Inghram, J. Drowart, in: Proceedings of an International Symposium on High Temperature Technology, McGraw-Hill, New York, (1960), pp. 219–240.
[14] N.S. Chilingarov, E.V. Skokan, J.V. Rau, L.N. Sidorov, Russ. J. Phys. Chem. (English transl. from Zhurnal Fizicheskoi Khimii) 66 (1992) 1127–1133.
[15] G. Kiriakidis, N. Katsarakis, M. Bender, E. Gagaoudakis, V. Cimalla, Mater. Phys. Mech. 1 (2000) 83–97.